

A new Greenland digital elevation model derived from ICESat-2 during 2018-2019

Yubin Fan^{1,2,3}, Chang-Qing Ke^{1,2,3*}, Xiaoyi Shen^{1,2,3}

¹Jiangsu Provincial Key Laboratory of Geographic Information Science and Technology, Key Laboratory for Land Satellite Remote Sensing Applications of Ministry of Natural Resources, School of Geography and Ocean Science, Nanjing University, Nanjing, 210023 China.

²Collaborative Innovation Center of Novel Software Technology and Industrialization, Nanjing, 210023 China.

³Collaborative Innovation Center of South China Sea Studies, Nanjing, 210023 China.

Correspondence to: Chang-Qing Ke (kecq@nju.edu.cn)

Abstract. Greenland digital elevation models (DEMs) are indispensable to fieldwork, ice velocity calculations, and mass change estimations. Previous DEMs have provided reasonable estimations for the entire Greenland, but the time span of applied source data may lead to mass change estimation bias. To provide a DEM with a specific time-stamp, we applied approximately 5.8×10^8 ICESat-2 observations from November 2018 to November 2019 to generate a new DEM, including the ice sheet and glaciers in peripheral Greenland. A spatiotemporal model fit process was performed at 500 m, 1, 2, and 5 km grid cells separately, and the final DEM was posted at the modal resolution of 500 m. A total of 98% of the grids were obtained by the model fit, and the remaining DEM gaps were estimated via the ordinary Kriging interpolation method. Compared with IceBridge mission data acquired by the Airborne Topographic Mapper (ATM) Lidar system, the ICESat-2 DEM was estimated to have a maximum median difference of -0.48 m. The performance of the grids obtained by model fit and interpolation was similar, which both agreed well with the IceBridge data. DEM uncertainty rises in regions of low latitude and high slope or roughness. Furthermore, the ICESat-2 DEM showed significant accuracy improvements compared with other altimeter-derived DEMs, and the accuracy was comparable to those derived from stereo-photogrammetry and interferometry. Overall, the ICESat-2 DEM showed excellent accuracy stability under various topographic conditions, which can provide a specific time-stamped DEM with high accuracy that will be useful to study Greenland elevation and mass balance changes. The Greenland DEM and its uncertainty are available at <https://data.tpdc.ac.cn/en/disallow/07497631-0475-48b5-ba53-c17f9076c72f/> (Fan et al., 2021).

1 Introduction

Greenland's digital elevation model (DEM) is particularly important for fieldwork planning and numerical modelling verification (Bamber et al., 2009). The ice deformation rate and the underlying bedrock condition can be measured with ice thickness data, which is useful to determine subglacial hydrological pathways (Bamber et al., 2013). The surface elevation at different periods is also indispensable for studying elevation and mass changes to understand ice dynamics and estimate potential sea level changes (Sutterley et al., 2014; Smith et al., 2020). In addition, InSAR estimation of ice velocity requires

high-accuracy and up-to-date DEMs to distinguish phase differences caused by terrain and ice sheet movement (Riel et al., 2021).

35 The first published Greenland DEM can date back to the 1980s, providing elevations of peripheral Greenland generated through 3500 photographs from 1978 to 1987 with a resolution of 25 m (Korsgaard et al., 2016). However, the low-visibility contrast between snow and ice surfaces may affect the radiometric and geometric quality of stereoscopic DEMs (Noh and Howat, 2015), which may introduce considerable uncertainty to the elevation. Research regions were also restricted to the margin and outlets of Greenland, and there is a lack of understanding about the internal ice sheet.

40 The currently available DEMs of the entire Greenland include those based on stereo-photogrammetry, altimeters, and interferometry. Most DEMs were derived from stereo-photogrammetry images, such as the Greenland Ice Mapping Project (GIMP) DEM (version 1) derived from ASTER, SPOT 5, and AVHRR photogrammetry (Howat et al., 2014), GIMP2 and ArcticDEM derived from GeoEye-1 and WorldView-1/2/3. ArcticDEM was the latest released DEM, with the highest resolution (2 m) among all free available Greenland DEMs. Optical image pairs may be influenced by weather, clouds, and the solar elevation angle (Korona et al., 2009); thus, the posted DEM is the combination of images of long timespans, which 45 might limit its scientific applications to mass balance research. In addition, owing to the wide coverage (86°N-86°S), high single-point accuracy (0.1-0.15 m), and small footprint size (70 m) (Zwally et al., 2002), ICESat has the ability to measure the elevation of entire Greenland. Hence, a bi-quadratic surface to fit ICESat footprints within each 1 km grid was adopted to obtain the ICESat DEM, but the largest search radius of 20 km in the low-latitude regions to some extent limited the ability to describe the small-scale elevation patterns at the Greenland margin (DiMarzio et al. 2007). A Ku-band synthetic aperture 50 interferometric radar altimeter (SIRAL) carried by CryoSat-2 further increases the spatial coverage within 88°N-88°S. Although the footprint size (approximately 300 m) was larger than that of ICESat, the smaller cross-track distance (2.5 km) still ensures its ability to monitor the ice sheet (Wingham et al., 2002); thus, CryoSat-2 L1B data from 2011 to 2014 were applied to generate Cryosat-2 DEM through Kriging interpolation approach (Helm et al., 2014). Coarse cross-track resolution is the major limitation to applying laser altimeters to generate a DEM with finer resolution (<1 km) in Greenland. TanDEM- 55 X and TerraSAR-X were also used to generate the Greenland DEM using differential interferometry (Zink et al., 2014), but the X-band radar signal penetration depth into the dry snowpack may cause the elevation to be underestimated by several meters (Dehecq et al., 2016). These DEMs provide reasonable estimations for the entire Greenland, but the specific timestamps of the current DEMs were missing.

60 ICESat-2, a new generation of satellite-borne lidar altimeters, is intended as a successor to the ICESat mission to quantify the contribution of polar ice sheets to sea level rise and the impact of climate change (Markus et al., 2017). ICESat-2 has an orbital altitude of 500 km and an orbital inclination of 92°, accompanied by a revisit period of 91 days, and can provide centimetre-scale measurements of different surface types. The ICESat-2 beam footprint of approximately 17 m with a spatial interval of 0.7 m ensures accurate elevation measurements at a high orbital resolution by determining the local ice sheet slope (Neumann et al., 2019). A much finer observation can be obtained owing to its along-track distance of 0.7 m and cross-track distance of 65 3.3 km, which is a significant improvement compared with CryoSat-2's along-track distance of 0.3 km and cross-track distance

of 1.5 km, and ICESat's along-track distance of 170 m. Not only the resolution but also the accuracy has been improved. The accuracy in the flat ice sheet can reach 3 cm, and it can still be less than 14 cm even for complex topography (Shen et al., 2021), which makes ICESat-2 a great data source to generate a DEM with high resolution and accuracy.

70 Here, we present a novel Greenland DEM (ICESat-2 DEM) in May 2019 with a 500 m resolution using a spatiotemporal model fit based on ICESat-2 measurements from November 2018 to November 2019. The overall accuracy of ICESat-2 DEM was evaluated by comparing it to the spatiotemporally matched IceBridge data. The performance was also compared with other published DEMs under various terrain conditions to validate the reliability of the ICESat-2 DEM.

2 Data

2.1 ICESat-2 ATL06 data

75 The ICESat-2 land ice height product ATL06 (Release 003) was used here for DEM generation. The product provides longitude, latitude, and surface heights based on the WGS84 ellipsoid. The ATL06 product is developed from global geo-located photon data (ATL03) to estimate the land ice height (Smith et al., 2019). Compared with the original ATL03 product, land ice height is determined after instrument bias corrections (e.g., transmit pulse shape bias correction and first-photon bias correction) (Markus et al., 2017). The beam pair separation of the ATL06 product is set at 3.3 km across the track. The three pairs contain
80 one strong beam and one weak beam, and the two beams within each pair are separated by 90 m distance.

Brunt et al. (2019) compared the elevation of the ICESat-2 ATL06 product and GPS data and found that the accuracy differences of strong and weak beams are less than 2 cm. Shen et al. (2021) compared ICESat-2 ATL06 product with IceBridge data under complex terrain, and the results indicated that the height difference between them is also trivial. Hence, we included weak beams to increase spatial coverage and data point utilization because no systematic errors were found in strong and weak
85 beams in ICESat-2 elevation measurements. However, only data marked as good quality (`atl06_quality_summary=0`) were used for DEM generation to improve the accuracy of the DEM. Over the entire Greenland ice sheet and outlet glaciers, we used approximately 5.8×10^8 ICESat-2 elevation footprints to generate a new DEM, that is, the ICESat-2 DEM.

2.2 IceBridge data

To evaluate the accuracy of the ICESat-2 DEM, we used ATM surface elevation data from the IceBridge survey. ATM was
90 intended to fill the gap between ICESat and ICESat-2, working at the same wavelength (532 nm) as ICESat-2. The absolute elevation accuracy of the ATM system can reach 0.1 m, and the position accuracy on the flat ice sheet is less than 1 m (Kurtz et al., 2013). The IceBridge ATM L2 Icessn Elevation, Slope, and Roughness Version 2 dataset was used to evaluate the DEMs. The final resolution of IceBridge was resampled to 25 m, and the estimated error was approximately 12 cm (Krabill et al., 2004). The root-mean-square error (RMSE) was taken as the roughness of each IceBridge data. The slope and aspect of
95 IceBridge were described in Shen et al. (2021).

During 2009-2019, IceBridge provided millions of footprints over Greenland, covering both the peripheral and inland areas of Greenland. The distribution of IceBridge data for May 2019, which was used to evaluate the accuracy of the new ICESat-2 DEM, is displayed in Figure 1. We also calculated the histogram of the elevation, surface slope, surface aspect, and roughness of IceBridge in May 2019. Overall, the elevations of the sampled regions ranged from 0 m to 3500 m, the surface slopes ranged from 0° to 10°, the surface aspects ranged from 0° to 360°, and the roughnesses ranged from 0 cm to 20 cm (**Figure 2**). These sampled areas had variable surface terrain conditions, which provided a reliable dataset to evaluate the performance of the ICESat-2 DEM.

2.3 Other available Greenland DEMs

We used other published DEMs to compare the performance of the generated ICESat-2 DEM, and the detailed information concerning these DEMs is provided in Table 1, and all DEMs have been referenced to the WGS84 ellipsoid.

2.3.1 GLAS/ICESat 1 km Laser Altimetry DEM

Greenland's DEM, derived from GLAS/ICESat laser altimetry data (from February 2003 to June 2005), provides the surface elevation for both Greenland ice sheets and caps, with less impact on slopes compared with radar altimetry data such as EnviSat and ERS 1/2. The spatial resolution is 1 km. The horizontal coordinates are based on polar stereographic coordinates system.

2.3.2 ArcticDEM

ArcticDEM is a high-resolution, high-quality digital surface model (DSM) of the Arctic at different spatial resolutions (2 m, 10 m, 32 m, 100 m, 500 m, and 1000 m) and its temporal coverage is from 2015 to 2018. The mosaicked DEM results are compiled from the best quality strip DEMs, and the filtered ICESat altimetry data are applied to improve the absolute accuracy. The estimated accuracy is approximately 85 cm at a resolution of 100 m (Xing et al., 2020). We used the elevation products of 500 m and 1000 m for comparisons.

2.3.3 TanDEM-X DEM

The TanDEM-X DEM (TanDEM) is a global DEM with a resolution of 90 m provided by the German Aerospace Centre (DLR). Data collection was completed in 2015, and global DEM production was completed in 2016 and published in 2018. Different from previous datasets, it was generated by two X-band radar satellites (TanDEM-X and TerraSAR-X), which provides synchronous information to create a high-accuracy DEM about the Earth's land surface. The absolute horizontal and vertical accuracy is less than 10 m. The temporal coverage of the TanDEM data is mainly from 2011 to 2014.

2.3.4 CryoSat-2 DEM

CryoSat-2 L1B level data from January 2011 to January 2014 were used to provide the elevation of Greenland. Here, Helm et al. (2014) used waveform re-tracking to process LRM data and applied interferometry to process SARIn data, respectively. Besides, he also leveraged slope correction to improve original product elevation accuracy. The bias of the CryoSat-2 DEM was less than 1 m in flat regions and less than 4 m in rugged regions, showing similar performance to the other DEMs obtained by laser and radar altimeters.

3 Methods

3.1 DEM generation

We followed the method of Slater et al. (2018) to compute the elevation of Greenland, which is an iterative least-squares fit model to all the elevation measurements in each grid as a quadratic surface. This model is described by Equation (1).

$$h_i = h + a_0x + a_1y + a_2x^2 + a_3y^2 + a_4xy + \frac{dh}{dt}(t - t_{mid}) \quad (1)$$

where h_i is elevations derived from ICESat-2 measurement points in one grid, h represents the modelled elevation, and a_0 , a_1 , a_2 , a_3 , and a_4 are surface elevation fluctuations. dh/dt is the elevation change rate in the 13 months. t is the month difference between May 2019 and the ICESat-2 acquisition time. t_{mid} is the time of the mid timestamp (May 2019), and (x,y) are the coordinates in the polar stereographic projection.

We found that there were more voids in low-altitude areas due to the low density of ICESat-2 footprints during the procedure of Greenland DEM generation. Therefore, it is necessary to select a suitable spatial resolution to accomplish DEM with fewer gaps. DEM accumulated within 250 m grids only covered 15.38% of the Greenland area and 30% even at high latitudes; hence, we discarded this resolution for further processing. In contrast, a 500 m resolution increases overall coverage to 33% and nearly 70% at high latitudes (**Figure 3**). With a 1 and 2 km resolution, the proportion of calculated portions exceeds 90% in the regions that are north of 75°N (basins 1, 2, and 8). However, a 2 km resolution cannot obtain optimal coverage in low-elevation areas, while a 5 km resolution can further increase the coverage in the southern basins (basins 4, 5, and 6).

To reduce the effect of any poor fit, quality control was constrained in terms of data availability, quality, and rationality. We set the minimum number of grid points to 10 and the minimum timestamp to 2 months, which could ensure that enough measurements were contained in a grid cell to generate a reliable DEM. We assumed that the maximum elevation change is 10 m/yr and that its uncertainty cannot exceed 0.4 m/yr (Slater et al., 2018). Furthermore, we assumed that DEM uncertainty is less than 10 m and the maximum RMSE in each grid is 10 m. After this filter procedure, the elevation range is -500 m-3600 m and this result is feasible since it is within the elevation range of published Greenland DEM products.

150 After the aforementioned process, we have acquired Greenland DEM at four resolutions (500 m, 1 km, 2 km, and 5 km). However, these four types of DEMs all include void areas thus we need to incorporate them to obtain final Greenland DEM results with minimal gaps. First, we used Greenland DEM with 500 m resolution as our first DEM source. Afterwards, Greenland DEMs with 1 km, 2 km, and 5 km resolution were resampled to 500 m by applying a bilinear method to fill the gaps in this DEM and the finer resolution as our first option. Unavoidably, there are still some voids in the final Greenland
 155 DEM, but this has a minor impact on DEM accuracy. In this study, we described the unvoided area (98%) in the final Greenland DEM as ‘calculated grids’ and termed the rest (2%) as ‘interpolated grids’. For the rest, an ordinary kriging approach was used for interpolation. The ICESat-2 DEM was posted at a modal resolution of 500 m after gap filling and interpolation. A median filter of 2.5 km×2.5 km was applied to the posted ICESat-2 DEM to minimize the influence of different resolutions.

Here, we applied different methods to estimate ICESat-2 DEM uncertainties in calculated grids and interpolated grids. The
 160 elevation uncertainty of the calculated grids was calculated by Equation (2) based on MATLAB R2018a. For interpolated grid uncertainty estimation, we just used the kriging variance error calculated by ArcGIS 10.6. There is a 95.5 percent probability that the actual elevation at the grid is the predicted raster value ± two times the square root of the variance error of the corresponding cell by assuming the kriging errors are normally distributed. Hence, the two times the square root of the value in the variance error was taken as the elevation uncertainty in the interpolated grids (Equation (3)).

$$165 \text{ elevation uncertainty}_{\text{calculated grids}} = t(1-0.025, n-p) \times SE(b_i) \quad (2)$$

$$\text{elevation uncertainty}_{\text{interpolated grids}} = 2 \times \sqrt{\text{variance error}} \quad (3)$$

where b_i is the elevation, $SE(b_i)$ is the standard error of the elevation, $t(1-0.025, n-p)$ is the 95% percentile of t-distribution with $n-p$ degrees of freedom, n is the number of ICESat-2 measurements in one grid, p is the number of regression coefficients (i.e., 7), and variance error is kriging variance error.

170 The slope was calculated by the method of Horn et al. (1994), thus the slope uncertainty was calculated based on the law of propagation:

$$\text{slope uncertainty} = \sqrt{\sum_{i=1}^8 \left(\frac{\partial \text{slope}}{\partial e_i} \times \sigma e_i \right)^2} \quad (4)$$

where σe_i is the elevation uncertainties of the adjacent grids of the central grid.

3.2 DEM accuracy evaluation

175 One ICESat-2 DEM grid cell usually has several IceBridge measurement points. In each grid cell, the ICESat-2 DEM elevation values were subtracted from the median of all IceBridge elevations within it, and this difference was seen as the final bias. Subsequently, we used the median difference (MED), the mean difference (MD), the median absolute difference (MAD), the standard deviation (STD), the RMSE, and the correlation (R) to evaluate each DEM. The calculations are as follows:

$$dh = \text{median}(\text{IceBridge}) - \text{DEM} \quad (5)$$

$$180 \quad \text{MED} = \text{median}(dh_i) \quad (6)$$

$$\text{MD} = \frac{1}{n} \sum_{i=1}^n dh_i \quad (7)$$

$$\text{MAD} = \text{median}(|dh_i|) \quad (8)$$

$$185 \quad \text{STD} = \sqrt{\frac{\sum_{i=1}^n (dh_i - \text{MD})^2}{n-1}} \quad (9)$$

$$\text{RMSE} = \sqrt{\frac{\sum_{i=1}^n dh_i^2}{n-1}} \quad (10)$$

where dh_i is the elevation difference in each DEM grid and n is the number of overlapping IceBridge footprints.

We additionally used elevation intervals of 0 m to 500 m, 500 m to 1000 m, 1000 m to 1500 m, 1500 m to 2000 m, and ≥ 2000 m to study the relationship between the elevation difference and elevation. For the surface slope, we divided the slope into 5 intervals of 0° to 0.25° , 0.25° to 0.5° , 0.5° to 1° , 1° to 2° , and $\geq 2^\circ$ to detect the relationship between the elevation difference and slope. Similarly, the same step was repeated for roughness intervals of 0 cm to 5 cm, 5 cm to 10 cm, 10 cm to 15 cm, 15 cm to 20 cm, and ≥ 20 cm. We identified the aspect as north, east, south, and west to investigate the relationship between the elevation difference and terrain aspect.

4. Results

195 4.1 General attributes of ICESat-2 DEM

Approximately 33.00%, 23.93%, and 25.43% of elevations were directly estimated from Greenland DEM at 500 m, 1 km, and 2 km resolutions, corresponding to the number of ICESat-2 footprints of 3.51×10^8 , 3.96×10^8 , and 4.50×10^8 , respectively. The ICESat-2 DEM shows the same pattern as the other published DEMs. The highest elevation appears in the ice sheets and shows a downward trend to the margins (**Figure 4 (a)**), and large topographic fluctuations occur on the outlet glaciers around the periphery of Greenland. Furthermore, the monthly elevation change rate was also obtained from spatiotemporal model fit, thus the DEM for each month from November 2018 to November 2019 can be derived theoretically.

The DEM uncertainty and slope uncertainty show obvious latitude-dependent patterns. Larger values tend to be found at low latitudes, and this pattern may be related to the number of ICESat-2 measurement points in each grid cell. The uncertainty also presents an increasing trend from the interior to the margins, which is approximately less than 0.5 m in the inner ice sheet and higher uncertainty of 2-5 m can be observed for the periphery of Greenland (**Figure 4 (b)**). The generated slope uncertainty is large at the edges, which is also concurrent with slopes exceeding 1° (**Figure 4(c) and 4(d)**). The accuracy of satellite laser altimeters is affected by surface roughness, slope, and other environmental factors (Brunet et al., 2017). A flatter surface

provides a more uniform reflection than a steeper surface of the measurement footprint, and more accurate height measurements of the original ICESat-2 footprints can be obtained in the low-slope regions, hence the higher accuracy of the
210 ICESat-2 DEM.

4.2 Evaluation of ICESat-2 DEM by comparing with IceBridge data

The ICESat-2 DEM compares favourably to the IceBridge data (**Figure 5 and Table 2**). The bias between Greenland DEM and IceBridge data in calculated grids is smaller than that of interpolated grids, which indicates that the elevations derived
215 from model fit tend to be more accurate than those estimated from interpolation. Poorer performance in the interpolated grids is reasonable due to the low spatial correlation in the regions with large surface fluctuations such as the Greenland south margins. The application of four resolutions may add additional effects, i.e., different grid cell resolutions tend to present different elevation estimates; thus, DEMs of different resolutions (namely, 500 m, 1 km, 2 km, 5 km) were evaluated (**Table 3**). DEMs of 500 m and 1 km resolutions have similar performance, and DEMs with 2/5-km resolution exhibits worse
220 performances than those of 500 m and 1 km DEMs, but the biases of 2/5 km-resolution DEMs are still smaller than the error in the interpolated grid. Hence, it is reasonable to apply different resolutions for posting the ICESat-2 DEM of 500 m resolution considering the differences between the calculated and interpolated grids.

We also compared the accuracies according to the 10 basins covered by data from May 2019 (Table 4). The accuracy of the ICESat-2 DEM shows an apparent spatial trend in which better accuracy is observed in the north than in the south basins, and
225 the pattern may be related to the small proportion of calculated grids in the southern basin and the application of DEMs with 2 km and 5 km resolution. We calculated the mean elevation of main basins at four resolutions to further assess the effects of different spatial resolutions when generating the ICESat-2 DEM (**Figure 6**). The calculated elevations were generally higher with increasing resolution, and the regions with the largest bias were concentrated in the low-latitude basins of Greenland. The small elevation difference for the GLA region was possibly caused by the elevation being overestimated or underestimated on
230 different glaciers due to the complex topography, and this uncertainty alleviated the elevation differences.

There are still some differences between the ICESat-2 DEM and IceBridge data, mainly due to the inconsistent coverages of the two datasets. It should be noted that the IceBridge data used for evaluation were distributed only at latitudes below 75°N, where the posted DEM was mostly derived from DEMs at coarse resolutions. The ICESat-2 DEM should have higher accuracy in regions beyond 75°N. Hence, these biases are acceptable because the evaluated value represents the upper bound of the
235 ICESat-2 DEM bias, and the deviation should be smaller when considering ICESat-2 DEM as a whole.

5. Comparison with other available DEMs

The elevation differences between the new ICESat-2 DEM and the other five published DEMs show that DEMs usually perform better for low-slope regions (**Figure 7**). The ICESat-2 DEM is generally close to that of the 500 m ArcticDEM except in complex terrains, which can prove the great reliability of the ICESat-2 DEM. In particular, significant positive values can

240 be seen in the elevation difference between the ICESat-2 DEM and TanDEM on the Greenland ice sheet, which is assumed to be caused by X-band penetration into the snowpack. All the difference maps show significant negative values in the Jakobshavn Isbrae glacier, where experienced the greatest loss of the Greenland ice sheet (Smith et al., 2020). This phenomenon may reflect the real elevation changes during different DEM acquisition times.

In this study, we used only IceBridge data that overlapped with the corresponding DEM period to evaluate all DEMs' vertical
245 accuracies for the entire Greenland and areas with small elevation changes (-0.05~0.05 m/yr) (Smith et al, 2020). Results show that the ICESat-2 DEM showed significant improvements in accuracy compared with other altimeter-derived DEMs, and is also comparable to DEMs derived from stereo-photogrammetry and interferometry. Compared with the ICESat DEM derived from the 6.9×10^6 footprints and the CryoSat-2 DEM derived from the 7.5×10^6 footprints, approximately 80 times as many data points were used to generate the DEM, thus the finer-resolution of 500 m and higher accuracies can be obtained (**Tables 5 and**
250 **6**). The ICESat-2 DEM has the best performance with regard to the parameters except for the MED of the CryoSat-2 DEM. Contrary to expectations, there is no elevation underestimation in the CryoSat-2 DEM, possibly because slope and topographic corrections have been performed. TanDEM has less bias in the coastal region, this is possibly caused by that ICESat data have been used to calibrate the raw DEMs there (Wessel et al., 2016). Although model-based or empirical models can, to some extent, correct the penetration bias (Abdullahi et al., 2019), such correction in the ice sheet is generally restricted to the regional
255 scope (Wessel et al., 2021), thus significant elevation underestimations cannot be corrected and still exist.

The accuracy of the ICESat-2 DEM is higher than the 1 km ArcticDEM. The comparison of 500 m ArcticDEM and ICESat-2 DEM using the IceBridge of the year 2018 can draw the same conclusion that the performance of the ICESat-2 DEM is comparable to the 500 m ArcticDEM (**Table 7**). The MAD, STD, and RMSE are all larger than those of the 500 m ArcticDEM, and it is reasonable that stereo-photogrammetry can generate more consistent elevation estimations at the regional scale than
260 altimetry. Nevertheless, the ICESat-2 DEM is comparable to DEM and 500 m ArcticDEM when slopes are less than 1° , which occupies approximately 70% of Greenland. ICESat data were used to calibrate the ArcticDEM in both the horizontal and vertical directions to increase the accuracy of ArcticDEM, but the actual changes in the ice surface introduce additional uncertainties because ICESat data predate the ArcticDEM by almost 10 years. Besides, systematic errors among the ArcticDEM's different sensors may also affect its accuracy (Candela, 2017).

265 The median differences in surface slope and roughness for these DEMs illustrate that all their elevation biases become larger with increasing slope and roughness with the exception of TanDEM (**Figure 8(b) and 8(c)**). Larger elevation differences in high-slope regions are reasonable as satellite images have a much finer original spatial resolution (2 m) than ICESat-2. Furthermore, DEMs generated by stereo pairs have obvious directivity in terms of surface aspect (**Figure 8(d)**). The accuracy on the north slope is significantly lower, mainly due to the poor illumination condition of the images in the north direction.

270 **6. Conclusions**

A new digital elevation model of Greenland was provided based on the ICESat-2 observations acquired from November 2018 to November 2019. The DEM was posted at a modal resolution of 500 m. 98% of the grids were directly derived from a model-fit method, and an additional 2% were interpolated by the kriging method. The application of different resolutions can reduce the number of interpolated grids and bias in the elevation estimation. Compared with spatiotemporally matched elevation
275 measurements from the IceBridge data, we estimated the uncertainty with a median difference of -0.48 m for the entire Greenland, which represents the upper bound of the ICESat-2 DEM bias. The accuracy of the ICESat-2 DEM shows an apparent spatial trend, and better accuracy can be observed in the northern basins than in the southern basins owing to the denser coverage of ICESat-2 tracks in the high-latitude regions.

Compared with other published Greenland DEMs, i.e., the ICESat DEM, CryoSat-2 DEM, 1 km ArcticDEM, 500 m
280 ArcticDEM, and TanDEM, the ICESat-2 DEM maintains great accuracy stability under various topographic conditions. The ICESat-2 DEM is superior to the previous satellite altimeter-derived DEMs in both spatial resolution and elevation accuracy. Smaller elevation differences between ICESat-2 DEM and DEMs derived from stereo-photogrammetry and interferometry can imply the reliability of the ICESat-2 DEM. Although the uncertainties in the ICESat-2 DEM are affected by the ICESat-2 measurements themselves, and the DEM in the low-latitude regions was derived from the results of coarse spatial resolution,
285 the specific time-stamped ICESat-2 DEM can benefit studies of elevation change and mass balance in Greenland. More ICESat-2 data can be used to generate DEMs with higher resolution as more ICESat-2 observations become available, especially in the southernmost glaciers.

Data availability

The elevation and elevation uncertainty maps of Greenland can be downloaded from the National Tibetan Plateau/Third Pole
290 Environment Data Center, Institute of Tibetan Plateau Research, Chinese Academy of Sciences at (<https://data.tpc.ac.cn/en/disallow/07497631-0475-48b5-ba53-c17f9076c72f/>, Fan et al., 2021) during under review.

Author contributions

Yubin Fan performed the DEM generation and wrote the manuscript; Chang-Qing Ke contributed to the conception of the study and supervised the work. Xiaoyi Shen contributed to the discussion and advised on the comparison with IceBridge data.
295 All authors contributed to the discussion of the results and to the improvement of the manuscript.

Competing interests

The authors declare that they have no conflict of interest.

Acknowledgements

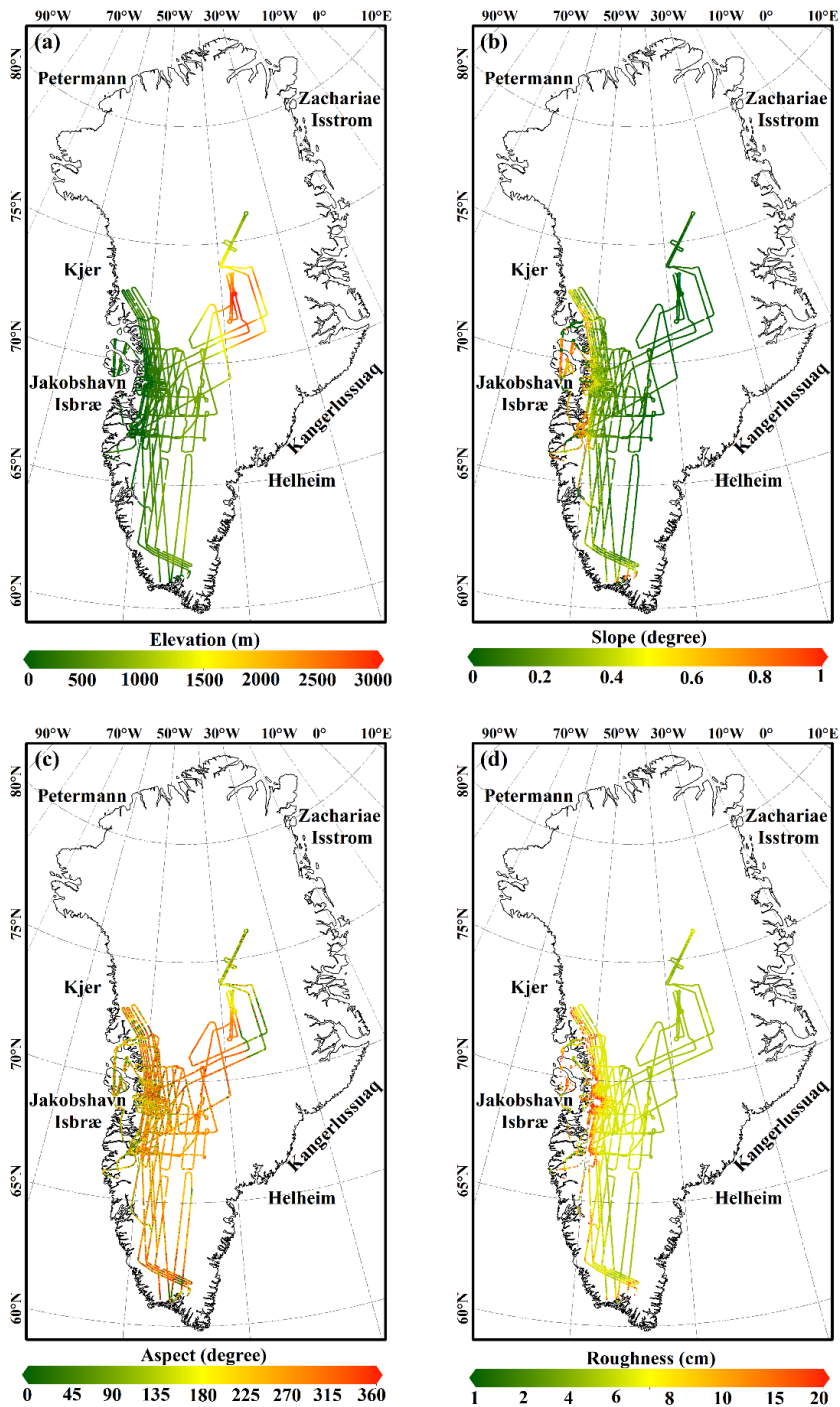
This work is supported by the Program for National Natural Science Foundation of China (grant No. 41830105). The ICESat-2 data were obtained from the National Snow and Ice Data Center (<http://nsidc.org>). We also thank the High Performance Computing Center, Nanjing University for the computing support.

References

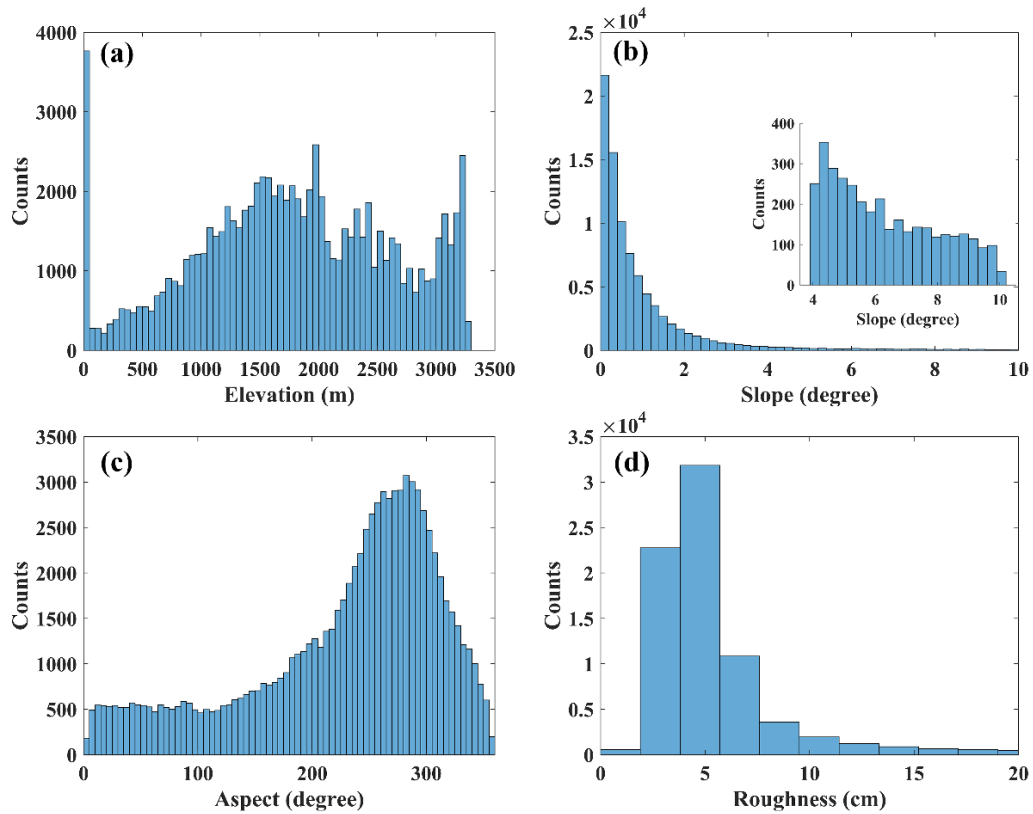
- Abdullahi, S., Wessel, B., Huber, M., Wendleder, A., and Kuenzer, C.: Estimating Penetration-Related X-Band InSAR Elevation Bias: A Study over the Greenland Ice Sheet, *Remote Sens.*, 11(24), <https://doi.org/10.3390/rs11242903>, 2019.
- 305 Bamber, J. L., Gomez-Dans, J. L., and Griggs, J. A.: A new 1 km digital elevation model of the Antarctic derived from combined satellite radar and laser data - Part 1: Data and methods, *Cryosphere*, 3, 101-111, <https://doi.org/10.5194/tc-3-101-2009>, 2009.
- Bamber, J. L., Griggs, J. A., Hurkmans, R. T. W. L., Dowdeswell, J. A., Gogineni, S. P., Howat, I., Mougintot, J., Padén, J., Palmer, S., Rignot, E., and Steinhage, D.: A new bed elevation dataset for Greenland, *Cryosphere*, 7, 499-510, <https://doi.org/10.5194/tc-7-499-2013>, 2013.
- 310 Brunt, K. M., Hawley, R. L., Lutz, E. R., Studinger, M., Sonntag, J. G., Hofton, M. A., Andrews, L. C., and Neumann, T. A.: Assessment of NASA airborne laser altimetry data using ground-based GPS data near Summit Station, Greenland, *Cryosphere*, 11, 681-692, <https://doi.org/10.5194/tc-11-681-2017>, 2017.
- Brunt, K. M., Neumann T. A., and Smith B. E.: Assessment of ICESat-2 Ice Sheet Surface Heights, Based on Comparisons Over the Interior of the Antarctic Ice Sheet, *Geophysical Research Letters*, 46, 13,072–13,078, <https://doi.org/10.1029/2019GL084886>, 2019.
- 315 Candela, S. G.: ArcticDEM Validation and Accuracy Assessment, Agü Fall Meeting, 2017.
- Dehecq, A., Millan, R., Berthier, E., Gourmelen, N., Trouvé, and E., Vionnet, V.: Elevation changes inferred from TanDEM-X data over the Mont-Blanc area: impact of the X-band interferometric bias. *IEEE J. Sel. Top. Appl. Earth Obs. Remote Sens.* 9, 3870-3882. <http://dx.doi.org/10.1109/JSTARS.2016.2581482>, 2016.
- DiMarzio, J.P.: GLAS/ICESat 1 km Laser Altimetry Digital Elevation Model of Greenland, Version 1. Boulder, Colorado USA. NASA National Snow and Ice Data Center Distributed Active Archive Center. https://doi.org/10.5067/FYMKT3GJE0T_M, 2007.
- Fan, Y., Ke, C., Shen, X.: A new Greenland digital elevation model derived from ICESat-2. National Tibetan Plateau Data Center, <https://data.tpdc.ac.cn/en/disallow/07497631-0475-48b5-ba53-c17f9076c72f/>, 2021.
- 325 Helm, V., Humbert, A., and Miller, H.: Elevation and elevation change of Greenland and Antarctica derived from CryoSat-2, *Cryosphere*, 8, 1539-1559, <https://doi.org/10.5194/tc-8-1539-2014>, 2014.
- Howat, I. M., Negrete, A., and Smith, B. E.: The Greenland Ice Mapping Project (GIMP) land classification and surface elevation data sets, *Cryosphere*, 8, 1509-1518, <https://doi.org/10.5194/tc-8-1509-2014>, 2014.

- 330 Korona, J., Berthier, E., Bernard, M., Remy, F., and Thouvenot, E.: SPIRIT. SPOT 5 stereoscopic survey of Polar Ice: Reference Images and Topographies during the fourth International Polar Year (2007-2009), *ISPRS J. Photogramm. Remote Sens.*, 64, 204-212, <https://doi.org/10.1016/j.isprsjprs.2008.10.005>, 2009.
- Korsgaard, N. J., Nuth, C., Khan, S. A., Kjeldsen, K. K., Bjork, A. A., Schomacker, A., and Kjaer, K. H.: Digital elevation model and orthophotographs of Greenland based on aerial photographs from 1978-1987, *Sci. Data*, 3, 15, <https://doi.org/10.1038/sdata.2016.32>, 2016.
- 335 Krabill, W., Hanna, E., Huybrechts, P., Abdalati, W., Cappelen, J., Csatho, B., Frederick, E., Manizade, S., Martin, C., Sonntag, J., Swift, R., Thomas, R., and Yungel, J.: Greenland Ice Sheet: Increased coastal thinning, *Geophys. Res. Lett.*, 31, 4, <https://doi.org/10.1029/2004gl021533>, 2004.
- Kurtz, N. T., Farrell, S. L., Studinger, M., Galin, N., Harbeck, J. P., Lindsay, R., Onana, V. D., Panzer, B., and Sonntag, J. G.: 340 Sea ice thickness, freeboard, and snow depth products from Operation IceBridge airborne data, *Cryosphere*, 7, 1035-1056, <https://doi.org/10.5194/tc-7-1035-2013>, 2013.
- Markus, T., Neumann, T., Martino, A., Abdalati, W., Brunt, K., Csatho, B., Farrell, S., Fricker, H., Gardner, A., Harding, D., Jasinski, M., Kwok, R., Magruder, L., Lubin, D., Luthcke, S., Morison, J., Nelson, R., Neuenschwander, A., Palm, S., Popescu, S., Shum, C. K., Schutz, B. E., Smith, B., Yang, Y. K., and Zwally, J.: The Ice, Cloud, and land Elevation Satellite-2 (IC 345 ESat-2): Science requirements, concept, and implementation, *Remote Sens. Environ.*, 190, 260-273, <https://doi.org/10.1016/j.rse.2016.12.029>, 2017.
- Neumann, T. A., Martino, A. J., Markus, T., Bae, S., Bock, M. R., Brenner, A. C., Brunt, K. M., Cavanaugh, J., Fernandes, S. T., Hancock, D. W., Harbeck, K., Lee, J., Kurtz, N. T., Luers, P. J., Luthcke, S. B., Magruder, L., Pennington, T. A., Ramos-Izquierdo, L., Rebold, T., Skoog, J., and Thomas, T. C.: The Ice, Cloud, and Land Elevation Satellite-2 mission: A global geol 350 ocated photon product derived from the Advanced Topographic Laser Altimeter System, *Remote Sens. Environ.*, 233, 16, <https://doi.org/10.1016/j.rse.2019.111325>, 2019.
- Noh, M. J. and Howat, I. M.: Automated stereo-photogrammetric DEM generation at high latitudes: Surface Extraction with TIN-based Search-space Minimization (SETSM) validation and demonstration over glaciated regions, *GISci. Remote Sens.*, 52, 198-217, <https://doi.org/10.1080/15481603.2015.1008621>, 2015.
- 355 Riel, B., Minchew, B., and Joughin, I.: Observing traveling waves in glaciers with remote sensing: new flexible time series methods and application to Sermeq Kujalleq (Jakobshavn Isbrx), Greenland, *Cryosphere*, 15, 407-429, <https://doi.org/10.5194/tc-15-407-2021>, 2021.
- Shen, X. Y., Ke, C. Q., Yu, X. N., Cai, Y., and Fan, Y. B.: Evaluation of Ice, Cloud, And Land Elevation Satellite-2 (ICESat-2) land ice surface heights using Airborne Topographic Mapper (ATM) data in Antarctica, *Int. J. Remote Sens.*, 42, 2556-25 360 73, <https://doi.org/10.1080/01431161.2020.1856962>, 2021.
- Slater, T., Shepherd, A., McMillan, M., Muir, A., Gilbert, L., Hogg, A. E., Konrad, H., and Parrinello, T.: A new digital elevation model of Antarctica derived from CryoSat-2 altimetry, *Cryosphere*, 12, 1551-1562, <https://doi.org/10.5194/tc-12-1551-2018>, 2018.

- Smith, B., Fricker, H. A., Holschuh, N., Gardner, A. S., Adusumilli, S., Brunt, K. M., Csatho, B., Harbeck, K., Huth, A., Neumann, T., Nilsson, J., and Siegfried, M. R.: Land ice height-retrieval algorithm for NASA's ICESat-2 photon-counting laser altimeter, *Remote Sens. Environ.*, 233, 17, <https://doi.org/10.1016/j.rse.2019.111352>, 2019.
- Smith, B., Fricker, H. A., Gardner, A. S., Medley, B., Nilsson, J., Paolo, F. S., Holschuh, N., Adusumilli, S., Brunt, K., Csatho, B., Harbeck, K., Markus, T., Neumann, T., Siegfried, M. R., and Zwally, H. J.: Pervasive ice sheet mass loss reflects competing ocean and atmosphere processes, *Science*, 368, 1239-+, <https://doi.org/10.1126/science.aaz5845>, 2020.
- 370 Sutterley, T. C., Velicogna, I., Rignot, E., Mouginot, J., Flament, T., van den Broeke, M. R., van Wessem, J. M., and Reijmer, C. H.: Mass loss of the Amundsen Sea Embayment of West Antarctica from four independent techniques, *Geophys. Res. Lett.*, 41, 8421-8428, <https://doi.org/10.1002/2014gl061940>, 2014.
- Wessel, B., Bertram, A., Gruber, A., Bemm, S., and Dech, S.: A new high-resolution elevation model of Greenland derived from TanDEM-X, *ISPRS Annals of Photogrammetry, Remote Sensing and Spatial Information Sciences*, 2016.
- 375 Wessel, B., Huber, M., Wohlfart, C., Bertram, A., and Roth, A.: TanDEM-X PolarDEM 90 m of Antarctica: Generation and error characterization, *TC discussions*, 2021.
- Wingham, D. J., Ieee, Ieee, and Ieee: CryoSat: A mission to determine fluctuations in the Earth's ice fields, *Igarss 2002: Ieee International Geoscience and Remote Sensing Symposium and 24th Canadian Symposium on Remote Sensing, Vols I-Vi, Proceedings: Remote Sensing: Integrating Our View of the Planet*, Ieee, New York, 1750-1752 pp.2002.
- 380 Xing, Z. Y., Chi, Z. H., Yang, Y., Chen, S. Y., Huang, H. B., Cheng, X., and Hui, F. M.: Accuracy Evaluation of Four Greenland Digital Elevation Models (DEMs) and Assessment of River Network Extraction, *Remote Sens.*, 12, 24, <https://doi.org/10.3390/rs12203429>, 2020.
- Zink, M., Bachmann, M., Brautigam, B., Fritz, T., Hajsek, I., Krieger, G., Moreira, A., and Wessel, B.: TanDEM-X: The New Global DEM Takes Shape, *Ieee Geoscience and Remote Sensing Magazine*, 2, 8-23, <https://doi.org/10.1109/mgrs.2014.2318895>, 2014.
- 385 Zwally, H. J., Schutz, B., Abdalati, W., Abshire, J., Bentley, C., Brenner, A., Bufton, J., Dezio, J., Hancock, D., Harding, D., Herring, T., Minster, B., Quinn, K., Palm, S., Spinhirne, J., and Thomas, R.: ICESat's laser measurements of polar ice, atmosphere, ocean, and land, *J. Geodyn.*, 34, 405-445, [https://doi.org/10.1016/s0264-3707\(02\)00042-x](https://doi.org/10.1016/s0264-3707(02)00042-x), 2002.



390 Figure 1: IceBridge data acquired in May 2019, which were used to evaluate the generated ICESat-2 DEM, covering regions in Greenland with various terrain conditions: (a) elevation, (b) slope, (c) aspect, and (d) roughness. Labels in the picture are the main glaciers in Greenland.



395 **Figure 2: Histogram of the (a) surface height, (b) surface slope, (c) aspect, and (d) roughness derived from IceBridge data. The inset figure shows the histogram of surface slope between 4° and 10°.**

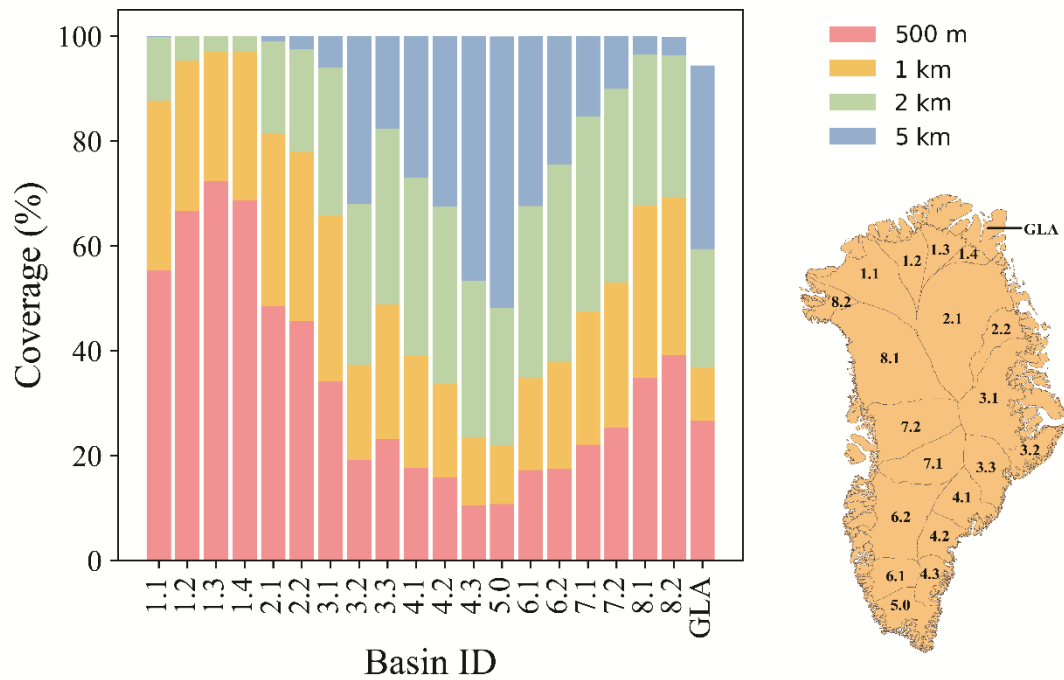


Figure 3: Coverage percentages of calculated elevation grids by ICESat-2 observations of 500 m, 1 km, 2 km, and 5 km. The basin boundaries are from Zwally et al. (2002), which divides Greenland into 8 main basins, covering approximately 1.72×10^6 km². Ice caps and glaciers that are not connected with the ice sheet are marked as GLA.

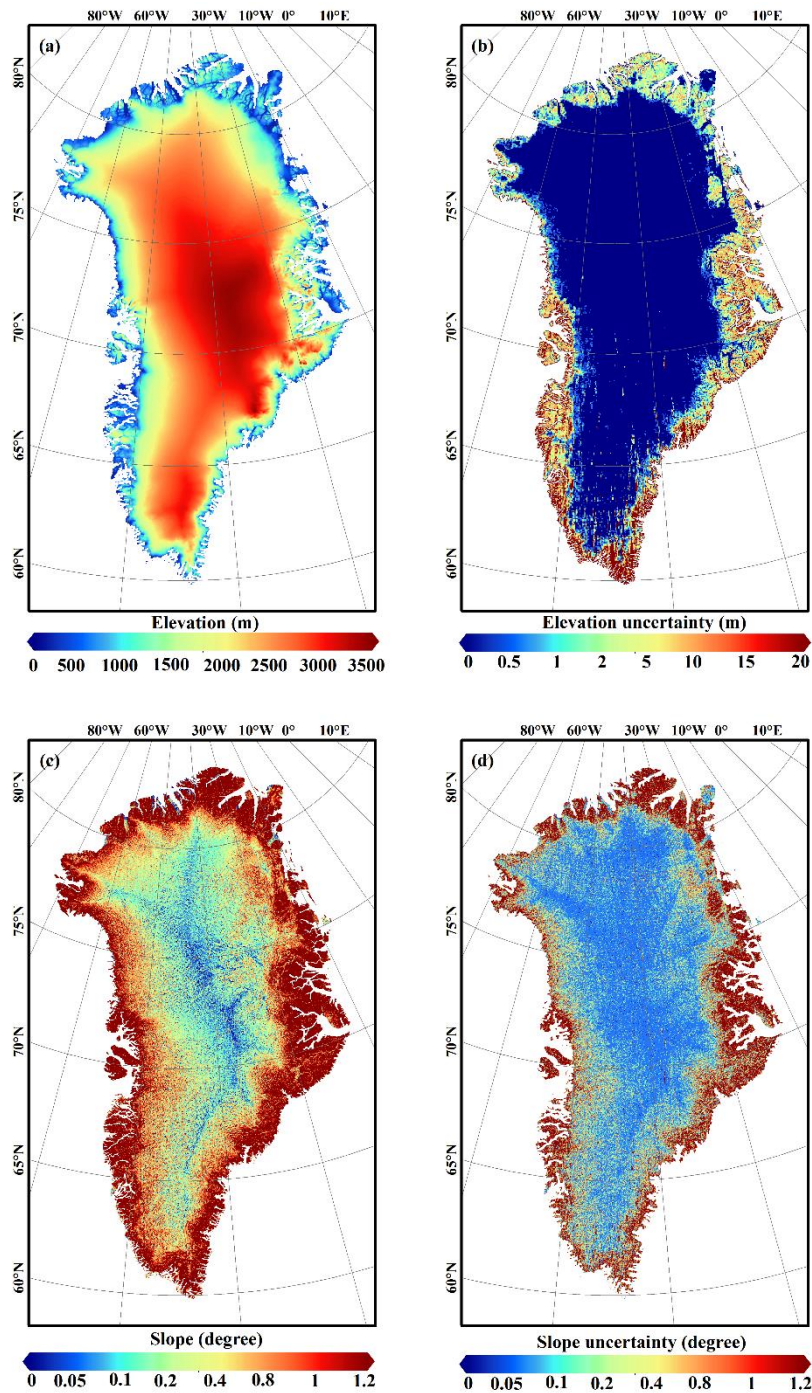
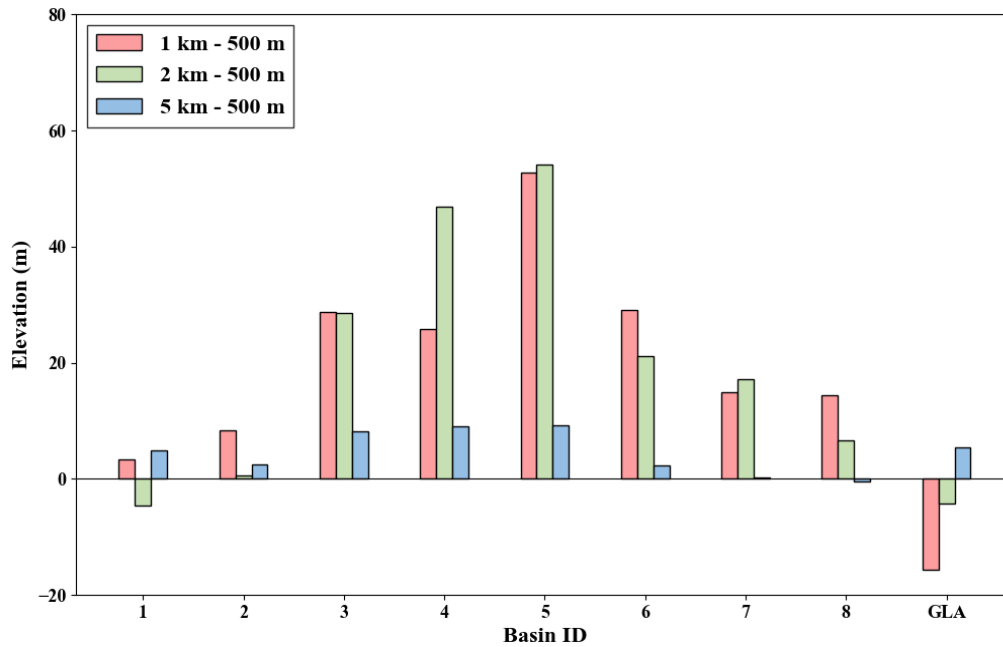
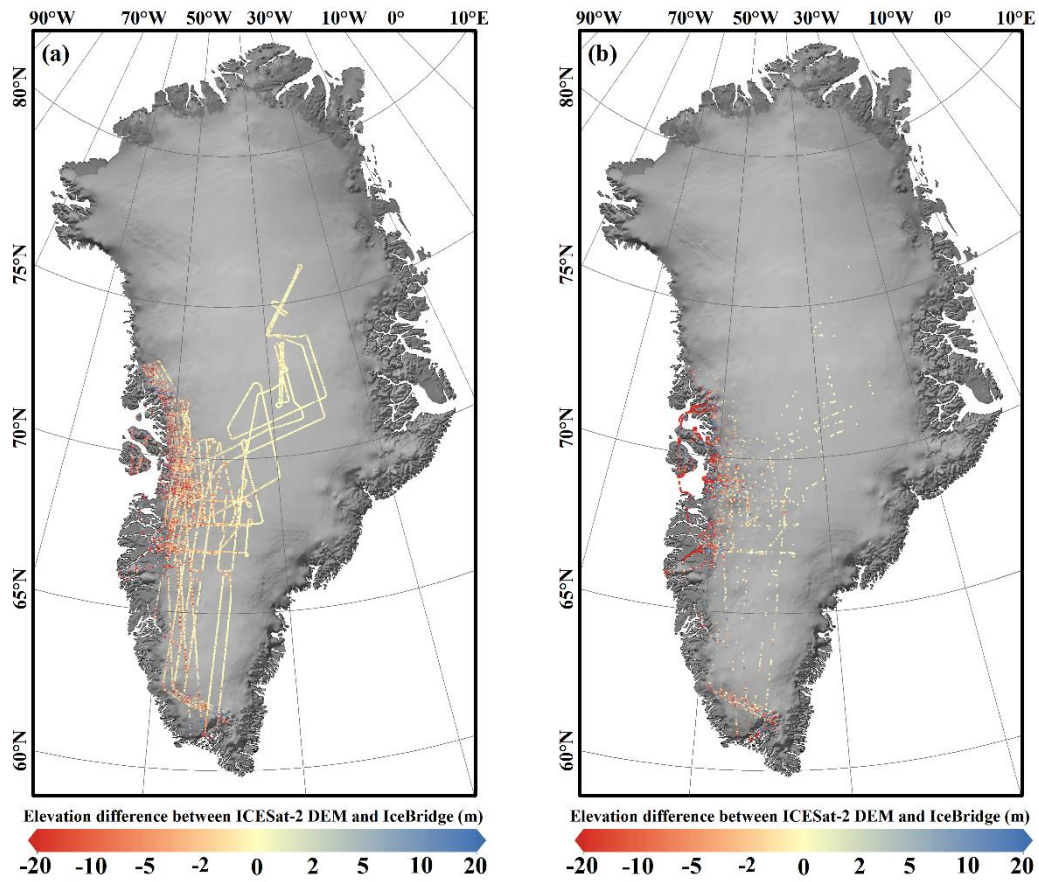


Figure 4: (a) Elevation of the Greenland DEM calculated from 13 months of ICESat-2 footprints acquired between November 2018 and November 2019. (b) The elevation uncertainties. (c) Slope derived from the elevation map (a) and (d) Slope uncertainty derived from the elevation map (b).



405 **Figure 5: Elevation differences of 9 main regions under different resolutions, which are calculated by subtracting the 500 m DEM from the 1 km, 2 km and 5 km DEM through the overlapping grids of different DEMs. The colour bar shows the mean elevation differences of these regions.**



410 **Figure 6: Elevation difference calculated as IceBridge data subtracted from the new ICESat-2 DEM. (a) Calculated grids and (b) interpolated grids. IceBridge data were acquired in May 2019.**

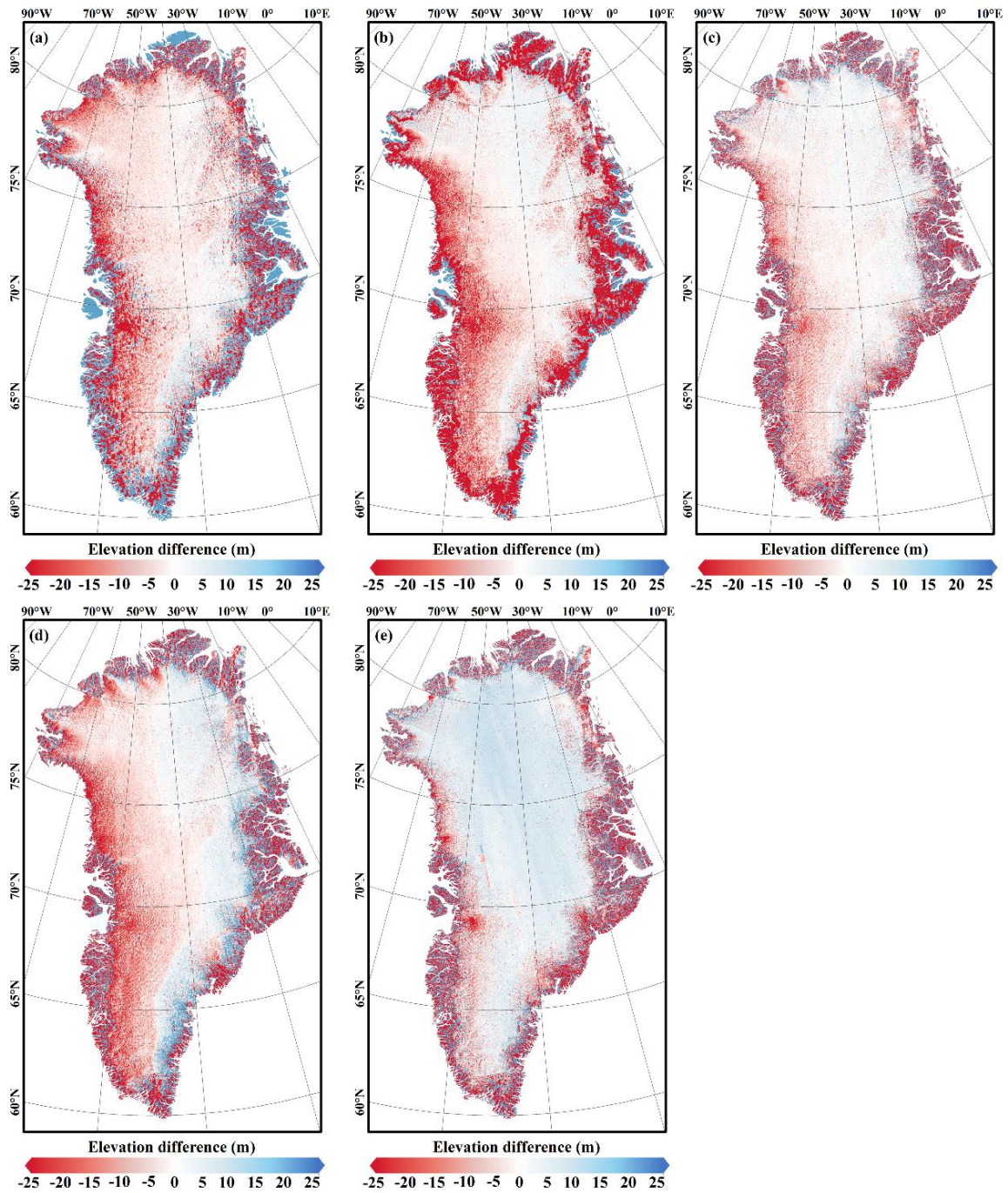


Figure 7: Elevation differences calculated between the new ICESat-2 DEM and the other five published available DEMs. (a) ICESat DEM, (b) CryoSat-2 DEM, (c) 500 m ArcticDEM, (d) 1 km ArcticDEM, and (e) TanDEM-X. For each picture, the previously published DEM was resampled to 500 m, and the difference was calculated as the resampled DEM subtracted from the new ICESat-2 DEM.

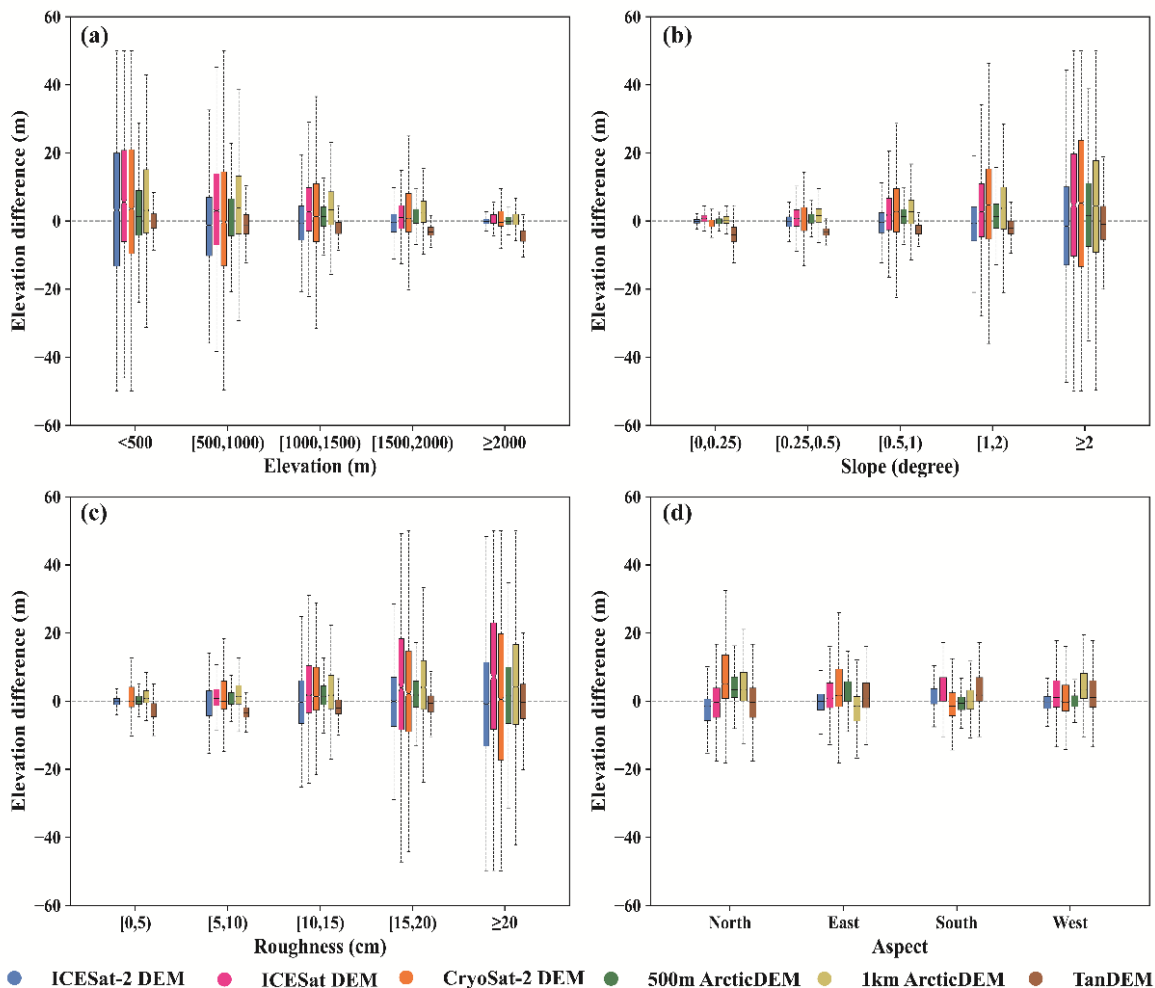


Figure 8: Elevation differences between different DEMs and IceBridge data under different terrain conditions. (a) Elevation, (b) slope, (c) roughness, and (d) aspect. The solid black lines near the box centres denote median values of elevation differences, the upper and lower boundaries of each box denote upper and lower quartiles (Q1 and Q3), the length means the interquartile range (IQR), and the top and bottom lines denote the range [Q1-1.5 IQR~Q3+1.5 IQR].

420

Table 1: Published Greenland DEMs used in this study. Note that the ArcticDEM has higher resolutions of 2, 10, 32, and 100 m and that we used only resolutions of 500 and 1000 m for comparison.

DEM	Data sources	Spatial coverage	Temporal coverage	Resolution (m)	DEM generation method
ICESat DEM	ICESat	99.99%	2003-2005	1000	bi-quadratic surface fit
ArcticDEM	GeoEye-1, WorldView-1, WorldView-2, WorldView-3	99.96% (500m), 99.98% (1000m)	2015-2018	500,1000	stereopair, calibrated by ICESat
TanDEM DEM	TanDEM-X, TerraSAR-X	99.93%	2011-2014	90	radar interferometry
CryoSat-2 DEM	CryoSat-2 AWI L2 data	99.33%	2011-2014	1000	Original kriging interpolation

425

Table 2: Elevation differences between the ICESat-2 DEM and IceBridge data for all of Greenland and the calculated and interpolated grids. IceBridge data were acquired in May 2019.

Region	MED (m)	MD (m)	MAD (m)	STD (m)	RMSE (m)	R	Number of compared grid cells
Total	-0.48	-1.90	2.73	11.31	11.47	0.9999	70046
Calculated grids	-0.48	-0.77	2.39	10.34	10.54	0.9999	61506
Interpolated grids	-0.48	-2.06	7.57	16.66	16.68	0.9998	8540

Table 3: Elevation differences between the ICESat-2 DEM and IceBridge data under different DEM resolutions.

DEM Resolution	MED (m)	MD (m)	MAD (m)	STD (m)	RMSE (m)	R	Number of compared grid cells
500m	-0.09	-0.16	0.60	2.55	2.55	0.9999	11186
1km	-0.01	-0.04	0.71	2.81	2.81	0.9999	6903
2km	-1.37	-1.78	2.52	6.34	6.59	0.9998	8453
5km	-0.72	-1.39	6.89	14.18	14.24	0.9998	245

430

Table 4: Elevation differences between the ICESat-2 DEM and IceBridge data in different basins, calculated for all of Greenland and the calculated and interpolated grids. Basins with fewer than 30 grids were excluded. IceBridge data were acquired in May 2019.

Basin	Region	MED (m)	MD (m)	MAD (m)	STD (m)	RMSE (m)	R	Number of compared grid cells
2.1	Total	0.20	-0.14	0.72	2.52	2.53	0.9999	4570
	Calculated	0.20	-0.15	0.71	2.53	2.53	0.9999	4525
	Interpolated	0.74	1.09	0.89	1.62	1.93	0.9999	45
3.1	Total	0.03	0.10	0.50	1.80	1.80	0.9997	2171
	Calculated	0.03	0.10	0.50	1.81	1.81	0.9997	2142
	Interpolated	-0.16	-0.22	0.27	0.58	0.62	1.0000	29
4.2	Total	0.12	0.12	0.40	1.44	1.44	0.9992	189
	Calculated	0.16	0.16	0.40	1.53	1.54	0.9991	158
	Interpolated	0.04	-0.05	0.31	0.76	0.74	0.9998	31
5	Total	-0.95	-0.22	5.11	12.92	12.92	0.9996	4965
	Calculated	-0.78	0.67	4.09	12.37	12.38	0.9997	3438
	Interpolated	-2.04	-2.21	7.35	13.90	14.07	0.9994	1527
6.1	Total	-0.34	-1.32	2.06	8.79	8.89	0.9998	4999
	Calculated	-0.34	-1.58	1.93	7.71	7.87	0.9999	4621
	Interpolated	-0.38	1.86	6.94	16.92	16.99	0.9997	378
6.2	Total	-0.87	-2.87	2.92	9.78	10.19	0.9999	25560
	Calculated	-0.91	-3.18	2.64	8.95	9.50	0.9999	22227
	Interpolated	-0.33	-0.75	5.98	13.90	13.92	0.9998	3333
7.1	Total	-0.63	-1.93	2.61	9.69	9.88	0.9999	15867
	Calculated	-0.65	-2.07	2.44	9.24	9.47	0.9999	14046
	Interpolated	-0.42	-0.85	4.82	12.62	12.64	0.9999	1821
7.2	Total	-0.53	-2.01	2.93	11.51	11.68	0.9999	19092
	Calculated	-0.54	-2.15	2.67	10.98	11.19	0.9999	17513
	Interpolated	-0.35	-0.41	8.00	16.18	16.18	0.9998	1579
8.1	Total	-0.87	-4.34	4.32	13.21	13.90	0.9999	1698
	Calculated	-0.89	-4.49	4.21	13.20	13.94	0.9999	1635
	Interpolated	-0.16	-0.34	7.41	12.76	12.66	0.9999	63
GLA	Total	-0.42	-0.77	17.15	24.14	24.15	0.9984	4891
	Calculated	-0.31	-0.70	14.79	22.54	22.55	0.9987	3254
	Interpolated	-0.90	-0.92	22.17	27.05	27.06	0.9970	1637

Table 5: Elevation differences of the ICESat-2 DEM and other published DEMs with respect to IceBridge data. The entire Greenland and regions with elevations above 2000 m and below 2000 m were compared.

	DEM	MED (m)	MD (m)	MAD (m)	STD (m)	RMSE (m)	R	Number of compared grid cells
Entire Greenland	ICESat-2 DEM	-0.48	-1.90	2.73	11.31	11.47	0.9999	70046
	ICESat DEM	1.02	2.15	3.66	13.22	13.40	0.9947	32106
	CryoSat-2 DEM	0.03	2.52	4.07	12.82	13.07	0.9679	113538
	500 m ArcticDEM	0.49	1.13	2.08	8.56	8.63	0.9994	346043
	1 km ArcticDEM	1.46	2.53	3.48	10.98	11.27	0.9988	151558
	TanDEM	-2.75	-1.78	3.19	6.33	6.58	0.9999	418676
Elevation above 2000 m	ICESat-2 DEM	-0.23	-0.63	0.97	4.63	4.67	0.9999	28321
	ICESat DEM	0.64	0.51	1.40	5.99	6.01	0.9979	11210
	CryoSat-2 DEM	-0.36	1.92	1.82	8.37	8.59	0.9873	46908
	500 m ArcticDEM	-0.07	0.40	0.97	3.26	3.28	0.9932	114165
	1 km ArcticDEM	0.33	0.32	1.52	5.27	5.28	0.9904	52155
	TanDEM	-3.76	-3.76	3.79	2.49	4.51	0.9999	83733
Elevation below 2000 m	ICESat-2 DEM	-1.32	-2.77	5.41	14.09	14.36	0.9996	41725
	ICESat DEM	1.97	3.03	6.49	15.72	16.01	0.9845	20896
	CryoSat-2 DEM	0.98	2.94	6.84	15.18	15.46	0.9062	66630
	500 m ArcticDEM	1.16	1.49	3.13	10.18	10.29	0.9992	231878
	1 km ArcticDEM	2.99	3.70	5.39	12.86	13.38	0.9980	99403
	TanDEM	-2.32	-1.29	3.00	6.88	7.00	0.9998	334943

440

Table 6: Elevation differences of the ICESat-2 DEM and other published DEMs with respect to IceBridge data in the regions which have little elevation change rate (-0.05 ~ 0.05 m/yr).

DEM	MED (m)	MD (m)	MAD (m)	STD (m)	RMSE (m)	R	Number of compared grid cells
ICESat-2 DEM	-0.20	-0.43	0.74	3.05	3.08	0.9999	15983
ICESat DEM	0.63	0.35	1.10	4.15	4.16	0.9999	6903
CryoSat-2 DEM	-0.63	0.87	1.42	6.05	6.11	0.9999	27268
500 m ArcticDEM	-0.14	0.04	0.77	2.19	2.19	0.9999	54235
1 km ArcticDEM	-0.04	0.06	0.82	2.67	2.67	0.9999	25675
TanDEM	-4.26	-4.43	4.26	1.97	4.85	0.9999	50656

445

Table 7: Elevation differences of the ICESat-2 DEM and 500m ArcticDEM with respect to IceBridge data in the entire Greenland and stable regions which have little elevation change rate (-0.05 ~ 0.05 m/yr).

Region	DEM							R	Number of compared grid cells
		MED (m)	MD (m)	MAD (m)	STD (m)	RMSE (m)			
Entire Greenland	ICESat-2 DEM	-0.24	-0.59	3.21	12.22	12.24	0.9999	90141	
	500m ArcticDEM	0.49	1.52	2.07	8.11	8.25	0.9999	90141	
Stable regions	ICESat-2 DEM	-0.11	-0.20	1.31	6.15	6.16	0.9999	22937	
	500m ArcticDEM	-0.19	-0.05	0.86	2.52	2.52	0.9999	22937	

450